Pergamon

Cement and Concrete Research, Vol. 25, No. 2, pp. 417-425, 1995

0008-8846/95 $9.50+.00

0008-8846(95)00027-5

PORE STRUCTURES OF FLY ASHES ACTIVATED BY $Ca(OH)_2$ AND $CaSO_4 \cdot 2H_2O$

Weiping Ma, Chunling Liu, Paul W. Brown* and Sridhar Komarneni**
Intercollege Materials Research Laboratory
The Pennsylvania State University
University Park, PA 16802

(Refereed)
(Received April 4; in final form November 9, 1994)

ABSTRACT

The nature of the pore structure which develops when low-lime fly ash reacts with $Ca(OH)_2$ and $CaSO_4 \cdot 2H_2O$ under hydrothermal treatment has been investigated. The nitrogen adsorption-desorption isotherms of hydrothermally treated samples of fly ash and activated fly ash were analyzed. X-ray diffractometry was used to characterize the hydration products and SEM was used to analyze microstructure. The shapes and sizes of the hysteresis loops of isotherms and the pore size distribution data indicated that the pore structures of samples were comprised primarily of wedge-shaped pores with open ends. The surface area obtained when fly ash reacted with $Ca(OH)_2$ under hydrothermal treatment at 100°C was 33.4 m^2/g, while that of untreated fly ash was only 1.3 m^2/g. The surface area of fly ash after reaction with $CaSO_4 \cdot 2H_2O$ was 2.9 m^2/g. For fly ash reacted with $Ca(OH)_2$, the volumes of the pores with radii of 19Å increased with increasing temperature of thermal treatment. Depending on the temperature, calcium silicate hydrate, calcite and anhydrite formed. Because the pozzolanic reaction produces calcium silicate hydrate with a very large surface area, it controls the pore structures in which fly ash is activated by $Ca(OH)_2$. Therefore, a realistic assessment of the pore structure of activated fly ash is needed to understand those important physical and mechanical properties of concrete.

Introduction

Fly ash is a heterogeneous material and can be used as a filler for rubber, as a filler in asphaltic shingles and asphaltic concrete, and used as a pozzolan in portland cement concrete. It has been widely used in concrete because partial replacement of portland cement by fly ash affects the temperature rise [1] and improves the workability of fresh concrete [2]. The chemical and mineralogical composition and the amount of fly ash substituted were found to decrease both the rate and the extent of heat generation [3]. Research by Ma et al. [4] on the hydration behavior of low-lime fly ash blended cement over the temperature range of 10° to 55°C at the early stage has shown that low-lime fly ash is relatively inert at these temperatures, and that its presence may actually retard the hydration of portland cement.

* also with the Department of Materials Science
** also with the Department of Agronomy

The reduction in strength gain associated with the presence of fly ash at the early stage indicates the need for an additional component to accelerate the hydration of low-lime fly ash [5]. Among the different ways of activating fly ash are the addition of $Ca(OH)_2$ or $CaSO_4 \cdot 2H_2O$. The possibility of fly ash activation by $Ca(OH)_2$ mainly lies in facilitating the pozzolanic reaction. This involves breaking of bonds and dissolution of the three-dimensional network structure of the glass [6,7]. It has been found previously that when $Ca(OH)_2$ is present, the solubility of SiO_2 in fly ash markedly increases [8,9]. The principle underlying activation by gypsum is based on the ability of the sulfate ions to react with aluminate, the latter being one of the principal components in fly ash. This also results in the dissociation of the glass structure [5].

It has been demonstrated that temperature affects both fly ash reactivity and the kinetics of dissolution [4,8,10]. In a model kinetic study of fly ash glass dissolution, Pietersen et al. [11] suggested that a significantly faster glass breakdown occurs at elevated temperature, and that it may cause a more rapid increase in the specific surface area. Moreover, Luxan et al. [12] pointed out that the treatment of fly ash with $Ca(OH)_2$ at elevated temperature may also cause the surface area to change.

It is generally agreed that the important engineering properties of concrete, such as strength, dimensional changes, and durability are primarily determined by the properties of the pore system of the hardened cement paste: the total surface area, the total pore volume, the pore size distribution and the pore connectivity [13,14]. Because the pozzolanic reaction produces calcium silicate hydrate with a very large surface area, it controls the pore structures in which fly ash is activated by $Ca(OH)_2$. Therefore, a realistic assessment of the pore structure of activated fly ash is needed to understand those important physical and mechanical properties of concrete.

Although studies have established the mechanism of hydration reactions between fly ash and $Ca(OH)_2$ or $CaSO_4 \cdot 2H_2O$, little appears to have been reported about the pore structure after hydrothermal treatment. Accordingly, in order to gain an insight into the effects of selective additions on the products formed by reaction with fly ash, surface areas and pore structure of the fly ash when activated under hydrothermal treatment were measured by a multipoint BET method. The hydration products were identified and characterized by X-ray diffractometry and scanning electron microscopy.

Experimental

The chemical composition of fly ash used in this study is as follows: SiO_2, 50.2%, Al_2O_3, 27.0%, Fe_2O_3, 13.8%, K_2O, 2.5%, CaO, 1.8%, TiO_2, 1.4%, MgO, 0.8%, P_2O_5, 0.5%. The loss on ignition at 1000°C is 1.71%. X-ray powder diffraction indicates that crystalline phases include quartz, mullite and hematite.

To prepare the samples for hydrothermal treatment, 3 g low-lime fly ash and 8 ml deionized water were mixed in the hydrothermal bomb. For activated fly ash, 10 wt.% $Ca(OH)_2$ or 10 wt.% $CaSO_4 \cdot 2H_2O$ of fly ash were added to the bomb before mixing. The samples were then treated hydrothermally for 24 hours at 100° and 180°C under saturated steam pressure using a tubular pressure vessel, and the vapor pressures are 15 and 145 psi, respectively. Reactions were also carried out at 25°, 60° and 80°C. After the treatment, the contents were transferred to a beaker and dried for 16 hours in an oven set at 60°C. Once completely dried, the samples were stored in a desiccator.

Nitrogen adsorption and desorption isotherms were measured using a Quantachrome Autosorb-1 Automatic Sorption Analyzer. The adsorption isotherm is the measurement of the quantity of gas adsorbed on a sample surface as the relative pressures increasing from 0 to 1 at constant temperature. Similarly, desorption isotherms can be obtained by measuring the quantities of gas removed from the sample as the relative pressure is lowered. The samples were degassed at 200°C before adsorption. Surface areas were calculated from the isotherm data using the BET (Brunauer-Emmett-Teller) equation in the relative pressure range of 0.008-0.3. A correlation coefficient of 1.0000 with a minimum of 5 points was achieved for all samples in the determination

of multipoint BET surface areas. The cross-section of nitrogen molecule was taken as 16.2Å^2. Pore size distributions were plotted using the BJH (Barrett-Joyner-Halenda) method. X-ray diffraction analyses were performed using CuKα1 radiation at a scan rate of 2° 2θ per minute. Microstructures were observed using an ISI-DS 130 dual stage scanning electron microscope.

Results and Discussion

Twelve samples were prepared for BET measurement. Seven of these adsorption-desorption isotherms are shown in figures 1 and 2. Figure 1 shows three types of hysteresis loops. Curve 1 is that of a sample prepared using low-lime fly ash, curve 2 is from ash reacted with 10 wt.% $Ca(OH)_2$ and curve 3 is from ash reacted with 10 wt.% $CaSO_4 \cdot 2H_2O$ at 25°C. The curves indicate the presence of macropores, shown by the sharp rise near P/P_o values of 1[15]. The hysteresis associated with the curves is the result of the difference in the free energy state of the adsorbed gas. At equivalent volumes of adsorbed gas, the desorption curves are at a lower pressure, and therefore the gas has a lower free energy state, and is closer to thermodynamic equilibrium [16]. The sizes and shapes of the hysteresis loops differ significantly depending the use of an activator. Low-lime fly ash has a small hysteresis loop, $CaSO_4 \cdot 2H_2O$ activated ash shows a larger loop, while activation of ash with $Ca(OH)_2$ produces the largest one. Nonetheless,the size and shapes of the three loops, shown in figure 1, indicate a continuous distribution of pore sizes. The shapes of the pores determine the shapes of the hysteresis loops.

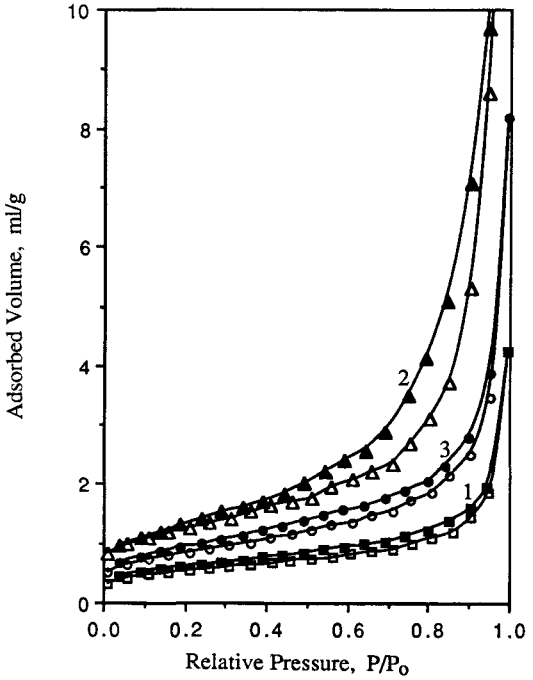

Figure 1. Nitrogen adsorption and desorption isotherms of samples hydrated for 24 hours at 25°C: (1) low-lime fly ash, (2) ash with 10 wt.% $Ca(OH)_2$ and (3) ash with 10 wt.% $CaSO_4 \cdot 2H_2O$. The open symbols are adsorption points, the filled symbols are desorption points.

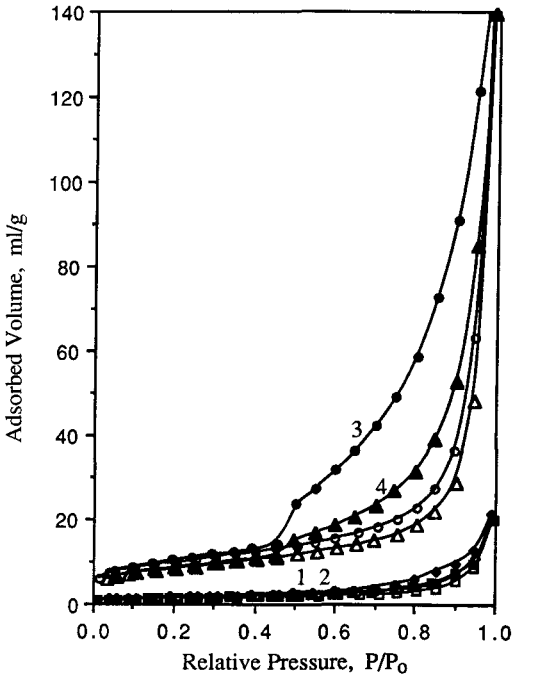

Figure 2. Nitrogen adsorption and desorption isotherms of fly ash with $Ca(OH)_2$ hydrothermally treated for 24 hours at (1) 25°C, (2) 60°C, (3) 100°C and (4) 180°C. The open symbols are adsorption points, the filled symbols are desorption points.

All of the hysteresis loops have a typical type C [17] shape corresponding to wedge-shaped pores with open ends. Hysteresis was slightly more pronounced in the activated samples, indicating a change in pore structure due to activation.

Comparing the isotherms of each set of samples reacted at elevated temperature, it was found that the curves for both untreated fly ash and $CaSO_4 \cdot 2H_2O$ activated fly ash at 25°C are almost identical. However, $Ca(OH)_2$ activated fly ashes show large changes in the shapes of their isotherms as the temperature of treatment increased. Figure 2 shows the isotherms of the low-lime fly ash reacted with $Ca(OH)_2$ for 24 hours at 25° and 60°C, and at 100° and 180°C under saturated steam pressure. As shown in Figure 2, each of the $Ca(OH)_2$ activated fly ash samples at elevated temperatures exhibits a BET type II isotherm (Brunauer classification [15]). This is indicative of unrestricted monolayer-multilayer adsorption. As the temperature increases, the isotherm hysteresis loops become larger. The sorption capacity at $P/P_0 > 0.99$ increases with reaction temperature up to 100°C. However, it is reduced when reaction occurs at 180°C. Again, the shapes of all hysteresis loops show that the samples have wedge-shaped pores with open ends.

Figure 3 shows the pore size distribution of low-lime fly ash reacted with 10 wt.% $Ca(OH)_2$ after hydration for 24 hours at various temperatures. The peak positions do not change with temperature, but the probabilities in the pore radius changed significantly. The volume in pores having radii of about 19Å increased with increasing temperature between 60° and 100°C. A much larger percentage of the pore volume is in this size range at 100°C than at 25° and 60°C.

Figure 3 also shows that hydration at 100°C produced an increased volume of pores over the range from 19Å to almost 0.1 μm. However, after hydration at 180°C there is a decrease in porosity in this size range. This is likely the result of the collapse of both micropores and mesopores. Because the surface area is developed almost exclusively as a result of the small pores, pore collapse would be responsible for the decrease in surface area at 180°C. The surface areas developed as a result of hydration vary as a function of temperature (Figure 4) in accord with the pore sizes observed in figure 3. The surface areas of fly ash hydrated with $Ca(OH)_2$ at 100° and 180°C are 33.4 and 29.7 m^2/g, respectively, while that of fly ash is 1.3 m^2/g and that of fly ash hydrated with $CaSO_4 \cdot 2H_2O$ is 2.9 m^2/g at 100°C.

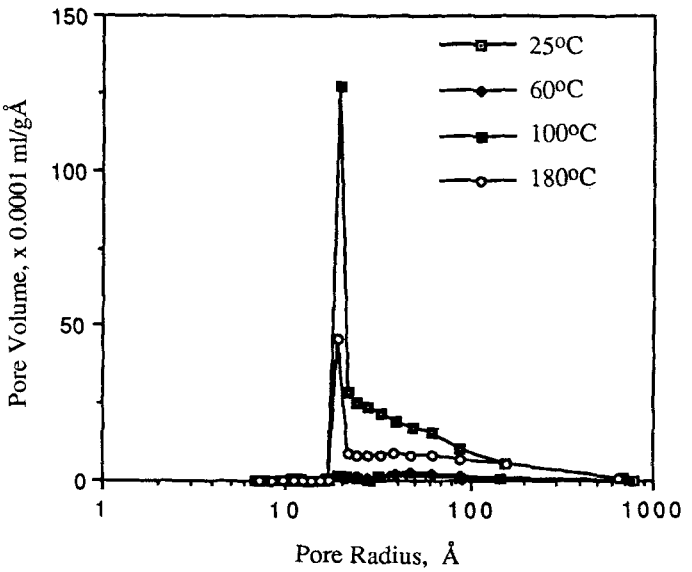

Figure 3. Pore size distribution for fly ash and $Ca(OH)_2$ mixture which was hydrothermally treated for 24 hours at 25, 60, 100 and 180°C.

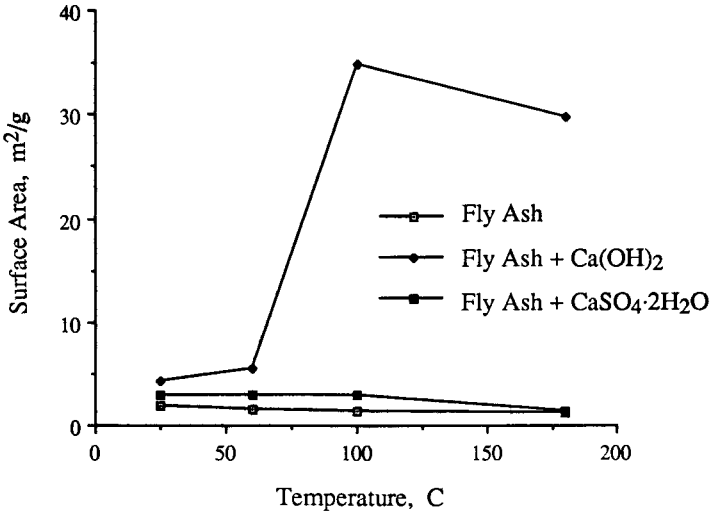

Figure 4. Nitrogen BET surface areas as a function of temperature of low-lime fly ash, ash with 10 wt.% $Ca(OH)_2$ and ash with 10 wt.% $CaSO_4 \cdot 2H_2O$, all hydrated for 24 hours.

Table 1 summarizes the multipoint BET surface areas and the nature of pore structures of the twelve samples analyzed. Low-lime fly ash develops surface areas ranging between 1.9 and 1.2 m^2/g at hydration temperature from 25° to 180°C. The surface area drops very slightly over this temperature range. Thus, it can be concluded that there is no significant effect of temperature on the surface area of this fly ash. Similarly, $CaSO_4 \cdot 2H_2O$ activated fly ash develops surface areas of 2.9 to 1.4 m^2/g. Temperature has the largest effect on the pore structure of fly ash hydrated with $Ca(OH)_2$. The surface area increased from 4.4 m^2/g at 25°C to 5.5 m^2/g at 60°C to 34.8 m^2/g at 100°C. Hydration at 180°C results in a surface area of 29.6 m^2/g. There are several kinds of pores with different pore size in low-lime fly ash, but their population is extremely low. As temperature increases, pores with an average radius of 11, 19 and 27 Å in size become more

TABLE 1.
Surface Areas, Pore Radii and Volumes and N_2 Sorption Capacities as a Function of Temperature of Fly Ashes Activated with $Ca(OH)_2$ or $CaSO_4 \cdot 2H_2O$

Samples	Temp. (°C)	Surface Area (m^2/g)	Pore Radius (Å)	Pore Volume (ml/g)	Sorption Capacity (ml/g)
FA	25	1.9	11, 15, 38	6.4×10^{-3}	4.3
FA	60	1.5	11, 19, 32, 60	6.2×10^{-3}	4.0
FA	100	1.3	11, 19, 27, 46	6.6×10^{-3}	4.2
FA	180	1.2	11, 19, 27, 60	5.4×10^{-3}	3.5
FA w/ C	25	4.4	12, 19, 47	3.1×10^{-2}	19.9
FA w/ C	60	5.5	12, 19, 47	3.3×10^{-2}	21.5
FA w/ C	100	34.8	19	2.9×10^{-1}	167.2
FA w/ C	180	29.7	19	2.2×10^{-1}	139.3
FA w/ S	25	2.9	8, 13, 32, 60	1.3×10^{-2}	8.2
FA w/ S	60	3.0	11, 19, 27	1.2×10^{-2}	7.9
FA w/ S	100	2.9	11, 19, 27	1.4×10^{-2}	9.0
FA w/ S	180	1.4	11, 19, 27	7.0×10^{-3}	4.5

FA - Fly ash, C - $Ca(OH)_2$, S - $CaSO_4 \cdot 2H_2O$

dominant. This effect is stronger in $CaSO_4 \cdot 2H_2O$ activated fly ash. The pore volume in $Ca(OH)_2$ activated fly ash is much higher. As temperature increases, the population of 19 Å pore increases quickly and eventually dominates the whole pore structure. It is observed that the pore volumes and sorption capacities are lower at 180°C than at 100°C in all instances because of pore collapse.

The probable cause of significant change of the surface area of fly ash hydrated with $Ca(OH)_2$ can be explained by X-ray diffraction analysis and scanning electron microscopy. The XRD patterns obtained (Figure 5 and 6) indicate that changes in both temperature and compositional variables result in the formation of a variety of phases. Partially unreacted fly ash can be observed due to the presence of quartz and mullite peaks after reactions with $Ca(OH)_2$ and $CaSO_4 \cdot 2H_2O$ at all temperatures. A number of crystalline phases were formed when the fly ash reacted with $Ca(OH)_2$ or $CaSO_4 \cdot 2H_2O$ as shown in figure 5 and 6, respectively. Calcite is observed after the treatment of mixtures of fly ash and $Ca(OH)_2$ regardless of temperature as shown in figure 5. Unreacted $Ca(OH)_2$ is present in samples hydrated at 25° and 60°C but disappears at 100° and 180°C. The presence of CSH is difficult to confirm by X-ray diffraction, because it is poorly crystalline and its main peak is masked by the main calcite peak. Figure 6 shows that calcium sulfate anhydrite, $CaSO_4$, was observed after hydrating the ash-$CaSO_4 \cdot 2H_2O$ mixtures at 180°C.

The surfaces of fly ash particles hydrated at elevated temperature were found to be smooth as observed by SEM, suggesting that no hydration occurred. Figure 7 compares the morphology of fly ash with 10 wt. % $Ca(OH)_2$ at 25° and 100°C, respectively. Fly ash shows poor reactivity with $Ca(OH)_2$ at 25°C, and most of the ash particles still retain their smooth surfaces. However, some products have needle-like morphologies and are suspected to be CSH, formed between the ash particles. Hydration with $Ca(OH)_2$ at 100°C resulted in the particles of fly ash becoming fully surrounded by CSH as shown in figure 7b. This observation is consistent with the development of high surface areas at 100°C compared with 25°C, as shown in figure 7a, because of the large surface of CSH. The observation of CSH is consistent with the study by Regourd [18], and the presence of such a CSH coating surrounding the fly ash particles is also consistent with a diffusionally controlled rate of reaction as discussed by Ma and Brown [9].

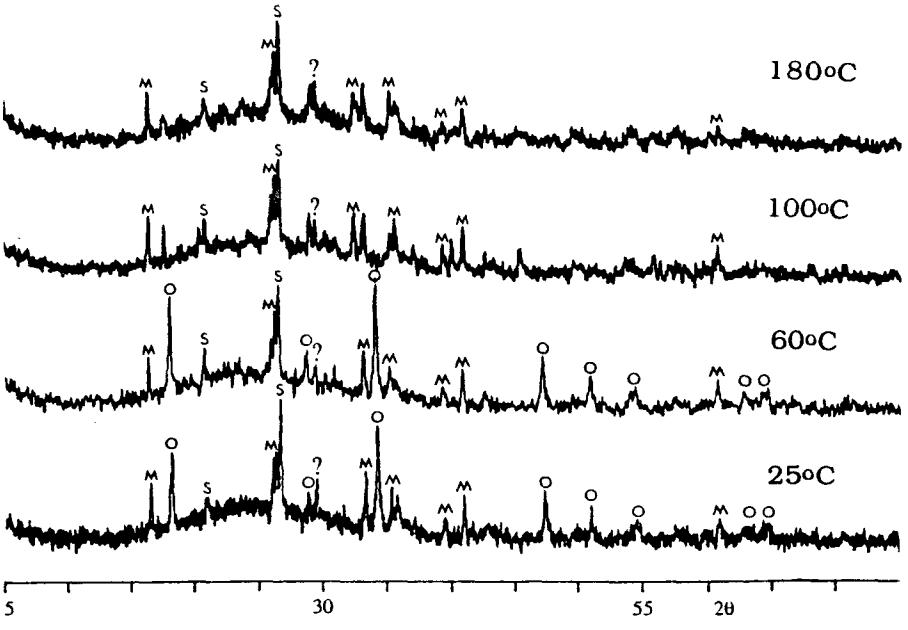

Figure 5. XRD patterns of fly ash and 10 wt.% $Ca(OH)_2$ mixtures which were treated at different temperatures for 24 hours. S - Quartz, M - Mullite, O - Calcium Hydroxide, ? - Calcium Silicate Hydrate or Calcite.

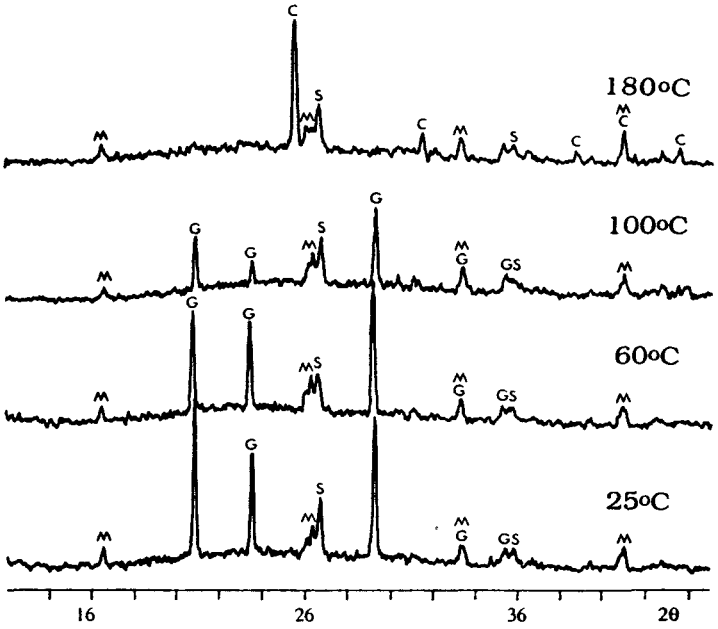

Figure 6. XRD patterns of fly ash and 10 wt.% $CaSO_4 \cdot 2H_2O$ mixtures which were treated at different temperatures for 24 hours. S - Quartz, M - Mullite, G - Gypsum, C - Anhydrite.

Figure 8 compares the morphology of hydration products which formed during the reaction of fly ash with 10 wt.% $CaSO_4 \cdot 2H_2O$ at 25° and 100°C for 24 hours. It can be seen from figure 8a that undissolved platy crystals of gypsum were readily identifiable in the pastes at 25°C. This suggests the poor reactivity of the fly ash at this temperature range. The reaction between fly ash and gypsum may be identified from the relic structure of gypsum crystals at 100°C, as shown in figure 8b. This reaction is not accompanied by the change of pore volume as discussed above.

Conclusions

The shapes and sizes of the hysteresis loops, as well as the pore data, indicate that a majority of fly ash and its mixtures with $Ca(OH)_2$ or $CaSO_4 \cdot 2H_2O$ contained primary wedge-shaped pores with open ends.

The volumes of pores having average radii of about 19Å increased with thermal treatment for low-lime fly ash with $Ca(OH)_2$, and the surface area increased as a result of treatment at elevated temperature. Calcium silicate hydrate was found to be responsible for the change of the surface area of fly ash with $Ca(OH)_2$ at elevated temperature. However, the effects on the pore volume and surface area for fly ash hydrated with gypsum in the temperature range of 25° to 180°C were minimal.

Acknowledgment

The authors gratefully acknowledge the support of U. S. Department of Energy, Grant DE-FG-22-91PC91302.

References

1. M. Tokyay, "Effects of Three Turkish Fly Ashes on the Heat of Hydration of PC-FA Pastes," Cem. Concr. Res., **18**, 957-60 (1988).

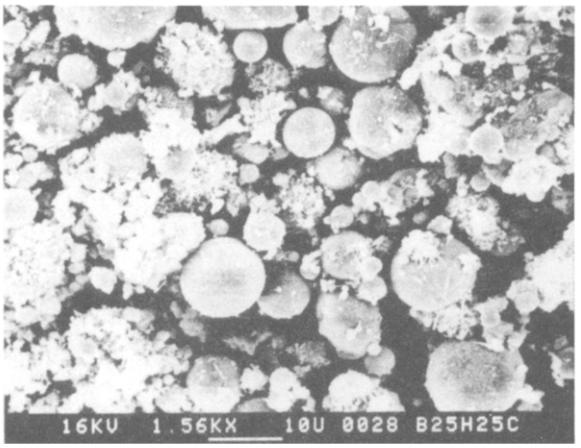

a

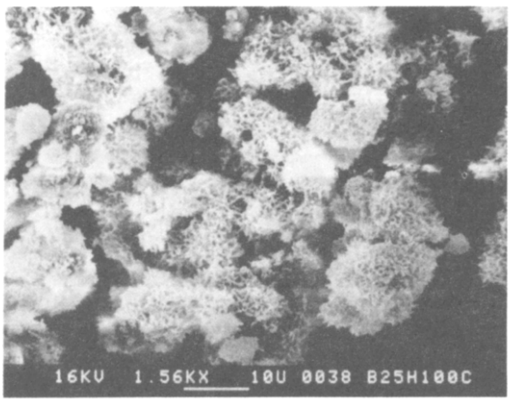

b

Figure 7. SEM images of fly ash and 10 wt.% $Ca(OH)_2$ mixture which was treated for 24 hours at (a) 25°C and (b) 100°C.

2. G. M. Idorn and K. R. Henriksen, "State of the Art for Fly Ash Uses in Concrete," Cem. Concr. Res., **14**, 463-70 (1984).
3. M. I. Sanchez de Rojas, M. P. Luxan, M. Frias and N. Garcia, "The Influence of Different Additions on Portland Cement Hydration Heat," Cem. Concr. Res., **23**, 46-54 (1993).
4. W. Ma, D. Sample, R. Martin and P. W. Brown, "Calorimetric Study of Cement Blends Containing Fly Ash, Silica Fume and Slag at Elevated Temperature," Cement, Concrete, and Aggregates, CCAGPD, **16**, 93-99 (1994).
5. X. Aimin and S. L. Sarker, "Microstructural Study of Gypsum Activated Fly Ash Hydration in Cement Paste," Cem. Concr. Res., **21**, 1137-147 (1991).
6. A. L. A. Fraay, J. M. Bijen and Y. M. de Haan, "The Reaction of Fly Ash in Concrete. A Critical Examination," Cem. Concr. Res., **19**, 235-46 (1989).
7. D. M. Roy and M. R. Silsbee, "Alkali Activated Cementitious Materials: An Overview," Mater. Res. Soc. Symp. Proc., **245**, 153-64 (1992).
8. R. O. Lokken, J. W. Shade and P. F. C. Martin, "Effect of Curing Temperature on the Properties of Cementitious Waste Forms," Mat. Res. Soc. Symp. Proc., **176**, 23-29 (1990).
9. P. W. Brown, "The System Na_2O-CaO-SiO_2-H_2O," J. Am. Ceram. Soc., **73**, 3457-63 (1986).
10. W. Ma and P. W. Brown, "Hydrothermal reactions of Fly Ash with $Ca(OH)_2$ and $CaSO_4 \cdot 2H_2O$" (in preparation).

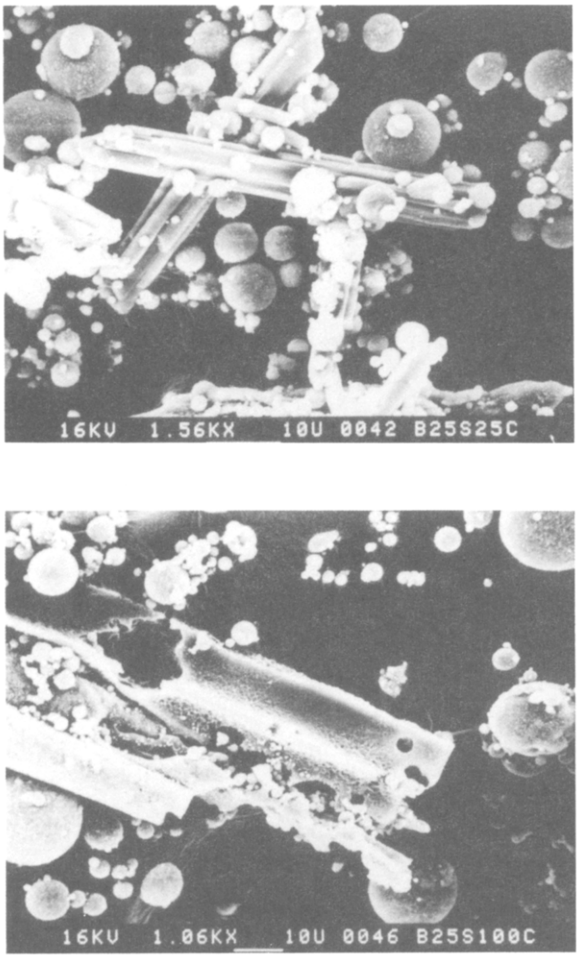

a

b

Figure 8. SEM images of fly ash and 10 wt.% $CaSO_4 \cdot 2H_2O$ mixture which was treated for 24 hours at (a) 25°C and (b) 100°C.

11. H. S. Pietersen, A. L. A. Fraay and J. M. Bijen "Reactivity of Fly Ash at High pH," Mat. Res. Soc. Symp. Proc., **178**, 139-157 (1990).
12. M. P. Luxan, M. I. Sanchez de Rojas and M. Frias, "Investigations on the Fly Ash-Calcium Hydroxide Reactions," Cem. Concr. Res., **19**, 69-80 (1989).
13. C. L. Kilgour, K. L. Bergeson and S. Schlorholtz, "Agglomeration of High Calcium Fly Ash for Utilization II. Binding Mechanisms," Mat. Res. Soc. Symp. Proc., **178**, 207-16 (1990).
14. E. E. Bodor, J. Skalny, S. Brunauer, J. Hagymassy, Jr. and M. Yudenfreund, "Pore Structures of Hydrated Calcium Silicates and Portland Cement by Nitrogen Adsorption," J. Colloid Interface Sci. **34**, 560-70 (1970).
15. S. Lowell and J. E. Shields, Powder Surface Area and Porosity, Third Edition, p 11-27, Chapman and Hall, New York, (1991).
16. P. J. Dewaele, E. J. Reardon and R. Dayal, "Permeability and Porosity Changes Associated with Cement Grout Carbonation," Cem. Concr. Res., **21**, 441-54 (1991).
17. J. H. deBoer's, The Structure and Properties of Porous Materials, p 68, Butterworths, London, (1958).
18. M. Regourd, "Microstructure of Cement Blended Containing Fly Ash, Silica Fume, Slag and Fillers," Mat. Res. Soc. Symp. Proc., **85**, 187-200 (1987).